Molecular Crystals and Liquid Crystals

ISSN: 1542-1406 (Print) 1563-5287 (Online) Journal homepage: http://www.tandfonline.com/loi/gmcl20

# Influence of DNA and DNA-PEDOT: PSS on dye sensitized solar cell performance

Cristiano C. Jayme, Jerzy Kanicki, François Kajzar, Ana F. Nogueira & Agnieszka Pawlicka

**To cite this article:** Cristiano C. Jayme, Jerzy Kanicki, François Kajzar, Ana F. Nogueira & Agnieszka Pawlicka (2016) Influence of DNA and DNA-PEDOT: PSS on dye sensitized solar cell performance, Molecular Crystals and Liquid Crystals, 627:1, 38-48, DOI: 10.1080/15421406.2015.1137680

**To link to this article:** http://dx.doi.org/10.1080/15421406.2015.1137680

Published online: 13 May 2016.

MOL. CRYST. LIQ. CRYST.
2016, VOL. 627, 38–48
http://dx.doi.org/10.1080/15421406.2015.1137680

Taylor & Francis
Taylor & Francis Group

# Influence of DNA and DNA-PEDOT: PSS on dye sensitized solar cell performance

Cristiano C. Jayme[a], Jerzy Kanicki[b], François Kajzar[c,d], Ana F. Nogueira[e], and Agnieszka Pawlicka[a,b]

[a]IQSC, Universidade de São Paulo, São Carlos, SP, Brazil; [b]EECS-University of Michigan, Ann Arbor, MI, USA; [c]Faculty of Applied Chemistry and Materials Science, University Politehnica of Bucharest, Bucharest, Romania; [d]Chemistry Laboratory, Ecole Normale Superieure of Lyon, Lyon, France; [e]Instituto de Química, UNICAMP, Campinas, SP, Brazil.

**ABSTRACT**

The present work shows the results of preparation, characterization, and application of DNA and DNA-PEDOT:PSS coatings as HTM in small dye sensitized solar cells. The samples were analyzed by impedance, UV-Vis and microscopic measurements. The measured ionic conductivities of the DNA membranes were of $2.5\times10^{-5}$ and $1.6\times10^{-3}$ S/cm at 25 and 75°C, respectively. The addition of PEDOT:PSS to the samples lowered the conductivities to $10^{-5}$ – $10^{-4}$ S/cm in the 25 – 75°C temperature range. The samples of DNA-PEDOT:PSS also showed lower transmittance as compared to pure DNA ones, which was due to their blue coloration. The addition of DNA and DNA-PEDOT:PSS as HTM in DSSC promoted a decrease of the device conversion efficiency, explained as due to the change of $TiO_2$-DNA morphology, increase of the device reflectance, and significant changes in device series and shunt resistances.

**KEYWORDS**

DNA; DNA-PEDOT:PSS; dye sensitized solar cells; solar energy conversion

## Introduction

The development of dye sensitized solar cells (DSSC) have attracted attention since presented by Oregan and Grätzel [1] in 1991. This interest is principally due to the possibility of their application as a new alternative for solar energy conversion. These electrochemical systems are considered as substitutes for expensive silicon-based solar energy conversion systems because they promise to be less expensive, can be semi-transparent and can operate up to 70°C, among others [2, 3].

The common DSSC has a sandwich structure with microporous, dye covered $TiO_2$, coating as photon caption layer, liquid or gel electrolyte with redox pair ($I^-/I_3^-$) and thin Pt coating as counter electrode [1, 4].

The efficiency of the DSSC can achieve almost 11% [4, 5]; however, it can be reached only for devices with liquid electrolytes that are problematic due to the evaporation and leakage [6]. Thus, gel or solid electrolytes seem to be a much better alternative for the liquid ones. However, the DSSCs with solid or gel electrolytes show lower conversion efficiencies when compared with DSSCs with liquid electrolytes, which is due to the

**CONTACT** Agnieszka Pawlicka agnieszka@iqsc.usp.br IQSC, Universidade de São Paulo, 13566-590, São Carlos, SP, Brazil
Color versions of one or more of the figures in the article can be found online at www.tandfonline.com/gmcl.

electrolyte-dye-$TiO_2$ poor contact [7]. Aiming to improve the charge transport between electrolyte and $TiO_2$–dye thin porous film and increase the efficiency of DSSC, the hole-transport materials (HTM) were applied on the top of $TiO_2$-dye. Among different HTMs that conduct holes are polyaniline, nickel or copper phtalocyanines, and poly(ethylene dioxythiophene):poly(styrene) (PEDOT:PSS) complex [8].

Deoxyribonucleic acid (DNA), which is one of several natural macromolecules, is not only highly abundant in our environment [9] but also very promising for electronic applications [10, 11]. It can be obtained either from plants or from animals, as for example from corn or salmon sperm [12]. Similarly to other natural macromolecules [13] it can easily form membranes with good mechanical properties and adhesion to glass and metal surfaces, and it also have a very good transparency [14, 15]. The macromolecular chains of DNA have a structure composed of heteroatoms, which could complex the lithium ions, protons or anions, or even release the sodium ions (the DNA is obtained in the sodium salt form), and thereby promote ionic conduction in these systems [16, 17]. It can also show ionic conduction properties in association with ionic liquids [18, 19].

The use of DNA in DSSC was shown by Bandyopadhyay *et al* [20], who reported about an all solid solar cells constituted of $TiO_2$ sensitized with *Rose Bengal* and DNA-based solid electrolyte. They found that depending on the type of DNA used, the short circuit currents in the DSSC increased between 200 and 400%. However, the performance of most investigated cells deteriorated after seven days of use. Some other few works report mostly on using DNA as scaffold for more effective $TiO_2$ coatings construction. Wang *et al* [21] prepared a novel 3D DNA-like $TiO_2$ structures that showed improvements in diffuse light capturing when compared with traditional microporous ones. Wire-like DNA-$TiO_2$ new nanomaterials were prepared and applied in DSSC by Nithiyanantham *et al* [22]. These DSSCs have shown the conversion efficiency of 2.47 and 3.03% depending on the size of the nanostructures. Zhang *et al* [23] prepared single wall nanotubes (SWNT)-$TiO_2$ and SWNT-$TiO_2$-Ag materials using DNA scaffold. The DSSC with these coatings revealed up to 5.99% of solar energy conversion efficiency.

Besides the works cited above, DNA was already investigated for electronics and photonics [24–26]. Some other reports present results of improvement in the electroluminescent properties of organic light emitting diodes (OLEDs) using modified DNA [27], and that DNA-CTMA layers basically possess both hole and electron transport abilities. It was also shown that these materials preferentially transport holes due to a shallow lowest unoccupied molecular orbital level (LUMO) that prohibits an efficient electron injection from an adjacent carrier transport layer [28].

Aiming to progress in DNA macromolecule applications, new membranes of DNA and DNA-PEDOT:PSS were prepared, characterized, and applied as HTM in small dye sensitized solar cells with FTO/$TiO_2$/dye/DNA/electrolyte/Pt configuration. The influence of DNA on DSSC solar energy conversion efficiency was analyzed throughout electrical, spectroscopic, and microscopic measurements.

## Experimental

1 g of DNA sodium salt ($DNA_O$; Ogata Research Laboratory, Chitose Institute of Technology, Japan) or acid ($DNA_A$; Aldrich®) was dissolved in 1000 mL of water Milli-Q®/etanol 1:1 solution for approximately 72 h. After complete dissolution of DNA, some small quantities were stored in hermetically closed glass flasks at room temperature. The rest was versed on Petri plates and cast for 72 h at room temperature until the complete dryness.

The samples of DNA-PEDOT:PSS were obtained by addition of PEDOT:PSS to the DNA solution described above. The PEDOT:PSS concentration was of 2, 5, 7, and 10% of DNA mass. The thickness of resulting membranes varied between $4.3\times10^{-3}$ and $4.9\times10^{-3}$ cm.

Complex impedance spectroscopy measurements were performed on membranes, having thickness of $4.3\times10^{-3}$ and $4.9\times10^{-3}$ cm, with the shape of discs sandwiched between two stainless-steel electrodes and placed under reduced pressure in a hermetically closed Teflon holder. Impedance data were collected with a Solartron model 1260 using an AC potential of 50 mV in the temperature range of 25 to 75°C and frequency range of 10 Hz–1 MHz.

Before the DSSC assembly, transparent and conducting glass/FTO (fluor tin oxide; Hartford; glass, $\leq$30 $\Omega/cm^2$) substrates were washed with water and detergent, and next cleaned in ultrasound bath for 15 min in acetone, isopropanol, ethanol, and distilled water each. Then the substrates were dried with dry $N_2$. Aiming to control the $TiO_2$ thickness, three layers of adhesive tape (Scotch Magic Tape 3M® with 50 μm of thickness) were glued parallel on both sides of glass/FTO substrate leaving 8 mm of distance between them. $TiO_2$ colloidal solution (Ti-Nanoxide T, Solaronix) was deposited by *doctor blading* method on glass/FTO substrates [2]. After drying in air for few minutes, the films were heat treated at 450°C for 30 min and at heating rate of 10°C/min in EDG3P – S owen resulting in about 30 μm thick films.

The glass/FTO/$TiO_2$-DNA or glass/FTO/$TiO_2$-DNA-PEDOT:PSS were obtained by dipping the glass/FTO/$TiO_2$ substrate in either DNA or DNA-PEDOT:PSS solution for 20 min. After that, these assemblies were covered with Petri plat for 2 min to promote better macromolecule penetration on $TiO_2$-dye microporous structure. Soon after, the samples were immersed in $1.0\times10^{-3}$ mol/L solution of hydrophobic TG6 dye [29] for 18 h. After that, some drops of polymer electrolyte based on poly(ethylene oxide-*co*-2-(2-methoxyethoxy) ethyl glicylether (P(EO/EM); Daiso); 70 wt% of $\gamma$-butirolactone; 5 wt% of LiI and $I_2$ [30] were placed on the top. Finally, counter-electrodes (CE), prepared by sputtering a thin Pt film (400 Rs$\leq$10 $\Omega/cm^2$) on FTO substrates, were pressed against the electrolyte coating. The DSSC devices with effective area of 0.25 $cm^2$ (inset Fig. 3) were characterized on an optical bench consisting of an Oriel Xe (Hg) 250 W lamp with intensity of 100 $mW/cm^2$, beam collimation lenses and filter AM 1.5. The light intensity was measured with a Newport Optical Power Meter 1830-C. Current–potential curves (I–V curves) were obtained using linear sweep voltammetry at 10 mV/s with the Eco Chimie-Autolab PGSTAT 10 potentiostat/galvanostat. The measurements were performed after 15 min of cell stabilization.

The UV–Vis spectroscopy measurements in transmittance mode of DNA and DNA-PEDOT:PSS liquid samples and using a 1 cm large quartz cubes were recorded with a Jasco 630V spectrophotometer between 190 and 1100 nm. The samples of in reflectance and absorbance mode of glass/FTO/$TiO_2$, glass/FTO/$TiO_2$/DNA, and glass/FTO/$TiO_2$/DNA-PEDOT:PSS were done between 400 and 800 nm.

The atomic force microscopy images (AFM) of glass/FTO/$TiO_2$, glass/FTO/$TiO_2$/DNA, and glass/FTO/$TiO_2$/DNA-PEDOT:PSS were taken with Nanosurf Easy Scan 2 AFM System (Nanosurf AG). The analyses were performed in contact mode using silicone tips with constant force of 0.2 N/m and resonance frequency of 13 kHz.

## Results and discussions

Aiming to study the ionic conducting membranes for dye sensitized solar cells (DSSC) new DNA-PEDOT samples were prepared and analyzed throughout electrochemical, spectroscopic, thermal, and microscopic analysis. Figure 1 shows the results of the ionic conductivity as a function of temperature evidencing an increase of conductivity with temperature for all

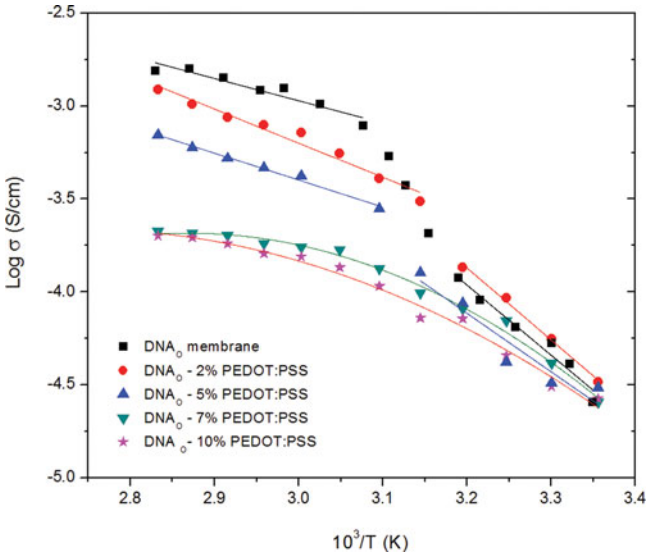


**Figure 1.** Log of ionic conductivity as a function of temperature of membranes of $DNA_0$ (■), $DNA_0$ – 2% PEDOT:PSS (●), $DNA_0$ – 5% PEDOT:PSS (▲), $DNA_0$ – 7% PEDOT:PSS (▼) and $DNA_0$ – 10% PEDOT:PSS (◀).

samples [31]. Figure 1 shows that up to 40°C all samples display very similar slight and linear increase of conductivity with temperature. At the 40 to 55°C temperature interval a sharp increase of conductivity occurs. After that, again a smooth increase of the ionic conductivity as a function of temperature is observed. This sharp increase of the conductivity of the samples of DNA and DNA-with 2 and 5% of PEDOT:PSS at 40 – 55°C can be result of DNA denaturation process [32, 33]. An addition of PEDOT:PSS to the DNA promotes a decrease of the ionic conductivity of the samples, differently to the DNA-PEDOT samples with plasticizer [26]. This decrease of the ionic conductivity, which is very clear above 50°C can be related to an increase of the crystallinity of the samples (not shown here) [34]. On the another hand, the samples with 7 and 10% of PEDOT:PSS don't display any abrupt change around 50°C. Only a Vogel-Tammann-Fulcher (VTF; Equation 1) behavior of log of ionic conductivity versus inverse of temperature is seen [35, 36], which means that the movement of charge carries is assisted by free volume of polymeric matrix [37]. Consequently, the quantity of the additive in the DNA matrix promotes a change in the ionic conductivity behavior from Arrhenius (Equation 2) to VTF, which was already observed in other natural macromolecular systems [38, 39].

$$\sigma = \sigma_0 T^{-\frac{1}{2}} exp\left(\frac{-B}{k(T - T_0)}\right), \tag{1}$$

$$\sigma = \sigma_0 exp\left(\frac{-E_a}{kT}\right), \tag{2}$$

where $\sigma_0$ is a pre-exponential factor proportional to the number of charge carries; $B$ is pseudo- and $E_a$ is activation energy for conduction (eV); $k = 8.6173 \times 10^{-5}$ eV/K is a Boltzmann constant; $T$ is the absolute temperature (K) and $T_o$ represents ideal vitreous transition temperature and it is suggested to be 50 K below the glass transition temperature ($T_g$).

The higher quantity of the PEDOT:PSS promotes probably stronger interaction with DNA by increasing the crystallinity of the system and decreases the ionic transport. This interaction can occur throughout electrostatic links as the macromolecules are polyelectrolytes.

**Table 1.** Ionic conductivities of $DNA_0$-based samples at 25 and 75°C.

| Sample | $\sigma$ (S/cm) at 25°C | $\sigma_m$ (S/cm) at 75°C |
|---|---|---|
| $DNA_0$ | $2.5\times10^{-5}$ | $1.6\times10^{-3}$ |
| $DNA_0$-2% PEDOT:PSS | $3.3\times10^{-5}$ | $1.0\times10^{-3}$ |
| $DNA_0$-5% PEDOT:PSS | $3.1\times10^{-5}$ | $6.0\times10^{-4}$ |
| $DNA_0$-7% PEDOT:PSS | $2.6\times10^{-5}$ | $2.1\times10^{-4}$ |
| $DNA_0$-10% PEDOT:PSS | $2.7\times10^{-5}$ | $2.0\times10^{-4}$ |

The ionic conductivities of the samples at room temperature and at 75°C, and measured with the purpose to evaluate their conducting properties are shown in Table 1. From data given in this table one can see that the ionic conductivity increases about two orders of magnitude for the DNA and DNA with 2% of PEDOT:PSS from about $10^{-5}$ to $10^{-3}$ S/cm and only one order of magnitude, i.e. to $10^{-4}$ S/cm for other three samples in the 25 to 75°C temperature range. It is important to note that the DNA-based ionic conducting membranes support such relatively high temperatures.

Aiming to analyze the transparency, the DNA and DNA-PEDO:PSS solutions were subjected to the UV-Vis-NIR analysis. Figure 2 shows that from 200 to 300 nm all samples are opaque and their transmittance increases with increase of the wavelength [26]. As expected, the DNA solution is the most transparent one when compared with other solutions achieving 70% at 550 nm and 80% at 600 nm. The transmittance of the DNA samples with PEDOT:PSS decreases with increasing dopant amount [26]. The transmittance of the sample of DNA with 2% of PEDOT:PSS is 65% at 550 nm and 52% for the sample with 10% of dye. However, at 730 nm almost all PEDOT:PSS containing samples have the transmittance of 67%. At larger wavelengths samples with higher quantity of dopant start to display higher transmittance values, which is probably due to the blue color of PEDOT:PSS.

Determination of current-voltage (I-V) curves is the most common and powerful method to characterize DSSC. From these curves, it is possible to obtain open circuit voltage ($V_{OC}$)

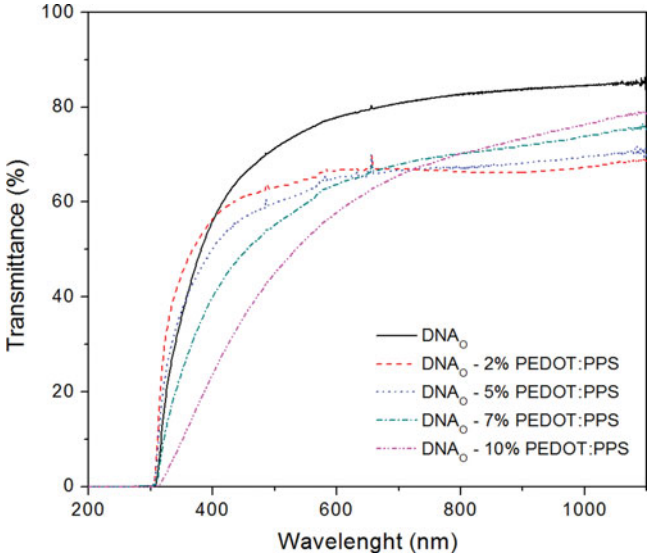


**Figure 2.** UV-Vis transmittance spectra of solutions of $DNA_0$ (—), $DNA_0$ — 2% PEDOT:PSS (-----), $DNA_0$ — 5% PEDOT:PSS (.....), $DNA_0$ — 7% PEDOT:PSS (_._._.) and $DNA_0$ — 10% PEDOT:PSS (_.._.._..).

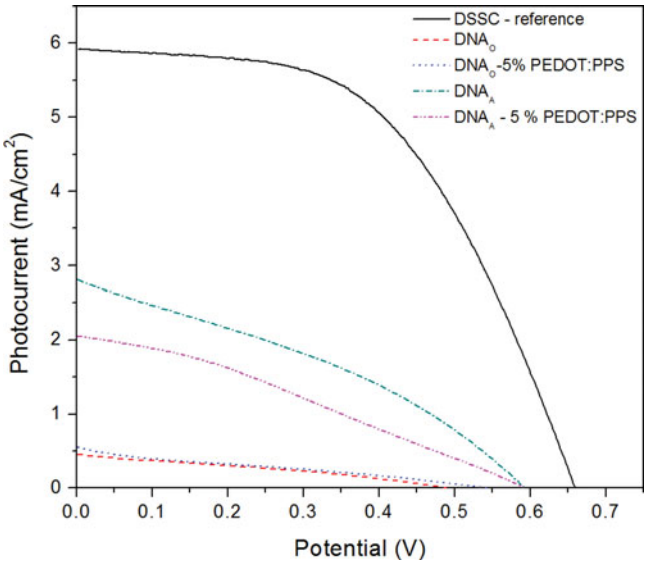


**Figure 3.** I versus V curves for DSSC reference and DSSC with $DNA_O$, $DNA_O$-5% PEDOT:PSS, $DNA_A$ and $DNA_A$-5% PEDOT:PSS.

and short circuit ($I_{SC}$), and from the shape of the I-V curve, it is possible to obtain conversion efficiency at any solar illuminations. Beside these parameters there are also others such as voltage ($V_{max}$) and current ($I_{max}$) at the maximum power, and fill factor (FF), which is a result of $V_{max} \times I_{max}$. Different DNA and DNA-PEDOT:PSS solutions were then applied as hole transport material (HTM) on glass/$TiO_2$ substrates (see experimental), which were next used to assemble small DSSCs. As reference, the conversion efficiency ($\eta$) of 2.04% for the DSSC with glass/$TiO_2$/dye/electrolyte/Pt configuration was obtained (Figure 3) [40]. The conversion efficiency values were obtained using the Equation (3).

$$\eta = \left(\frac{P_{max}}{P_{inc}}\right) x100\%, \tag{3}$$

where $P_{max}$ is a maximum power, $P_{inc}$ is power of incident light, which was 100 mW/cm$^2$ in present study.

Figure 3 shows that after addition of $DNA_O$ the efficiency of DSSC with $DNA_O$ decreased to 0.07%. Addition of PEDOT:PSS to DNA displayed the same low conversion efficiency as the device with $DNA_O$. Aiming to understand this phenomenon the high molecular weight $DNA_O$ was replaced by the low molecular weight $DNA_A$. The DSSC with $DNA_A$ revealed the efficiency value of 0.56%, which was higher than registered for DSSC with $DNA_O$ (Table 2).

**Table 2.** DSSC values of short circuit current ($J_{SC}$), open circuit potential ($V_{OC}$), fill factor (FF), efficiency ($\eta$) at 100 mW/cm$^2$ of light intensity, series ($R_s$) and shunt ($R_{sh}$) resistances.

| DSSC | $J_{sc}$ (mA/cm$^2$) | $V_{oc}$ (V) | FF (%) | $\eta$ (%) | $R_s$ ($\Omega^2$) | $R_{sh}$ ($\Omega^2$) |
|---|---|---|---|---|---|---|
| Reference | 5.91 | 0.66 | 52.33 | 2.04 | 35.99 | 2996.00 |
| $DNA_O$ | 0.46 | 0.49 | 30.72 | 0.07 | 611.57 | 617.53 |
| $DNA_O$-5% PEDOT:PSS | 0.56 | 0.54 | 25.13 | 0.08 | 102.94 | 210.03 |
| $DNA_A$ | 2.81 | 0.59 | 34.11 | 0.56 | 756.62 | 364.83 |
| $DNA_A$-5% PEDOT:PSS | 2.06 | 0.59 | 29.95 | 0.36 | 205.66 | 583.26 |

In both cases the addition of 5% of PEDOT:PSS to either $DNA_A$ or $DNA_O$ formulation did not improve the conversion efficiency that dropped to 0.37 and 0.07%, respectively.

The DSSC parameters such as short circuit current ($J_{SC}$), open circuit potential ($V_{OC}$), fill factor ($FF$), maximum power ($P_{max}$), and efficiency ($\eta$) at 100 mW/cm$^2$ are shown in Table 2. $P_{max}$ was the maximum value of $V_m$ and $J_m$ experimental values multiplication, and fill factor was calculated using the Equation (4).

$$FF = \frac{P_{max}}{P_{th}} = \frac{J_m x V_m}{J_{sc} x V_{oc}}, \tag{4}$$

where $P_{th}$ is a theoretical power; $V_m$ is a maximum potential, $J_m$ is a maximum current, $J_{SC}$ is a short circuit current, and $V_{OC}$ is an open circuit voltage.

As already mentioned above the best values of solar efficiency were obtained with $DNA_A$; however, these values were still lower when compared with the reference sample (Table 2). Beside this, it was observed that the DNA used in this research has a significant impact on the results. It seems that the low molecular mass $DNA_A$ purchased from Aldrich does not obstruct the charge transfer between electrolyte and $TiO_2$ as much as high molecular mass $DNA_O$ purchased from Ogata Institute (Figure 3).

The negative influence of the DNA-based HTM on the DSSC conversion efficiency can be due to (i) the reduction of the light absorption by the DSSC or (ii) changes in the sample's topography after DNA addition. The series ($R_s$) and shunt ($R_{sh}$) resistances as well as non-ideal diode parameters can also negatively influence the fill factor and consequently device performance [41]. The both resistances are called parasitic resistances, and they strongly depend on the geometry of the cell. For the ideal DSSC the $R_s = 0$ and $R_{sh} = \infty$.

The results shown in Table 2 show that the $R_s$ and $R_{sh}$ of the reference DSSC are 35.99 and 2996.00 Ω, respectively. Thus, they are low and high, which approaches to the ideal solar cell. Addition of DNA to the DSSC composition promoted an increase of $R_s$ to 611.57 and 756.62 Ω and a decrease of $R_{sh}$ to 617.53 and 364.83 Ω for the cells with $DNA_O$ and $DNA_A$, respectively. Further addition of PEDOT to DNA promoted a decrease of $R_s$ to 102.94 and 205.66 Ω for $DNA_O$- and $DNA_A$-5% PEDOT:PSS, respectively. This indicate an improvement of charge flow. However, at the same time the $R_{sh}$ of the cell with $DNA_O$-5% PEDOT:PSS decreased to 210.03 Ω, and of the cell with $DNA_A$-5% PEDOT:PSS increased to 583.26 Ω. Although, a decrease of $R_s$ and increase of $R_{sh}$ for the $DNA_A$-5% PEDOT:PSS should lead to a better solar efficiency values in present case the best $\eta$ was obtained for the DSSC with only $DNA_A$. This means that other factor such as a decrease of $TiO_2$-DNA effective area, coating thickness and porosity when compared with only $TiO_2$ can cause the efficiency decrease [42, 43].

The reduction of the light absorption of the DSSC with DNA coatings was then studied by UV-Vis spectroscopy. The measurements were performed with the samples of DNA deposited by dip-coating FTO/$TiO_2$ and measured in the reflectance mode using a principle of energy conservation given by the following Equation (5)

$$\frac{absorted\ light}{total} + \frac{reflected\ light}{total} + \frac{transmitted\ light}{total} = 1 \tag{5}$$

Figure 4 shows the results of reflectance measurements for the samples glass/FTO/$TiO_2$, glass/FTO/$TiO_2$/DNA and glass/FTO/$TiO_2$/DNA-PEDOT:PSS. The results, displayed in Figure 4a, show clearly that the addition of $DNA_A$ and $DNA_O$-PEDOT:PSS on the $TiO_2$ surface promoted an increase of the reflectance of the samples in whole 400 to 800 nm light range.

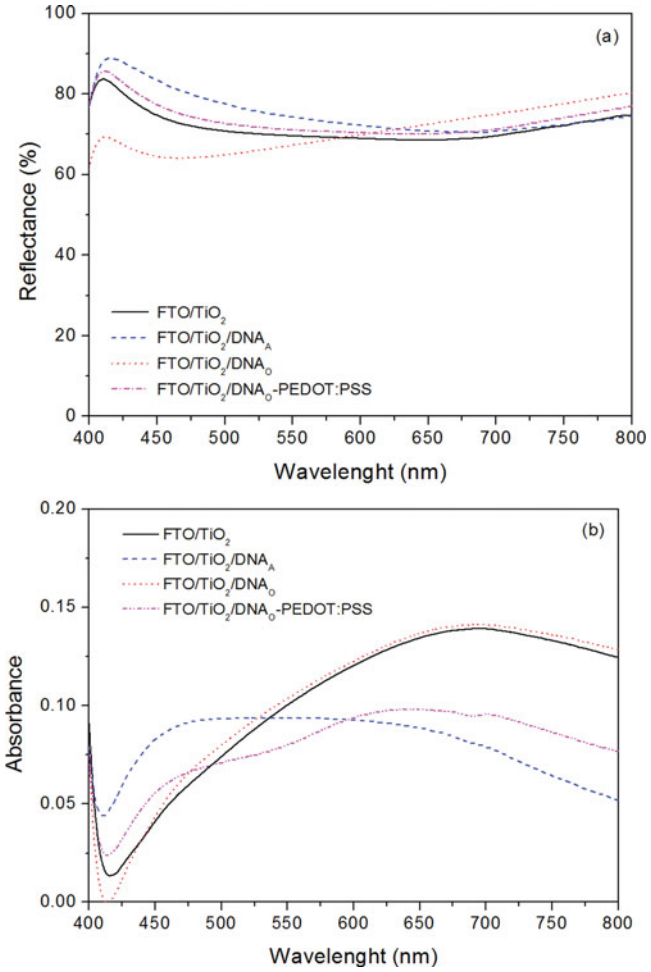


**Figure 4.** Reflectance (a) and absorbance (b) spectra of glass/FTO//$TiO_2$ (—·—·—), glass/FTO/$TiO_2$/$DNA_A$ (——), glass/FTO/$TiO_2$/$DNA_O$ (— —) and glass/FTO/$TiO_2$/$DNA_O$-5% PEDOT:PSS (···) samples.

As an example, the reflectance increased at 500 nm from 70% for glass/FTO/$TiO_2$ sample to 78 and 73% for glass/FTO/$TiO_2$/DNA and glass/FTO/$TiO_2$/DNA-PEDOT:PSS, respectively. This increase of the reflectance resulted in a decrease of the light absorption (Eq. 3), and consequently in the decrease of the DSSC conversion efficiency for wavelengths up to 630 nm. Figure 4a also shows that the sample with $DNA_O$ exhibits a lower reflectance as compared with other samples. However, at about 620 nm the reflectance starts to increase and at 650 nm is higher in comparison with other samples. An increase of reflectance probably leads to a decrease of absorbance, which results in a decrease of the DSSC efficiency [44]. Consequently, in the case of the sample with $DNA_O$ the improved absorption at lower wavelengths is canceled by poor absorption in higher wavelengths of the electromagnetic spectrum.

Analyzing the absorbance spectra in Figure 4b one can observe that the samples of FTO/$TiO_2$/$DNA_A$ show larger reflectance up to 550 nm when compared with other samples. Above this wavelength, the values start to decrease and at 600 nm are lower when compared with other samples. The $DNA_O$ - 5% PEDOT:PSS sample also shows a decrease of the absorbance at 500 nm, but at 600 nm its absorbance is larger in comparison with the $DNA_A$ sample. The values of absorbance confirm those of reflectance and the hypothesis that an

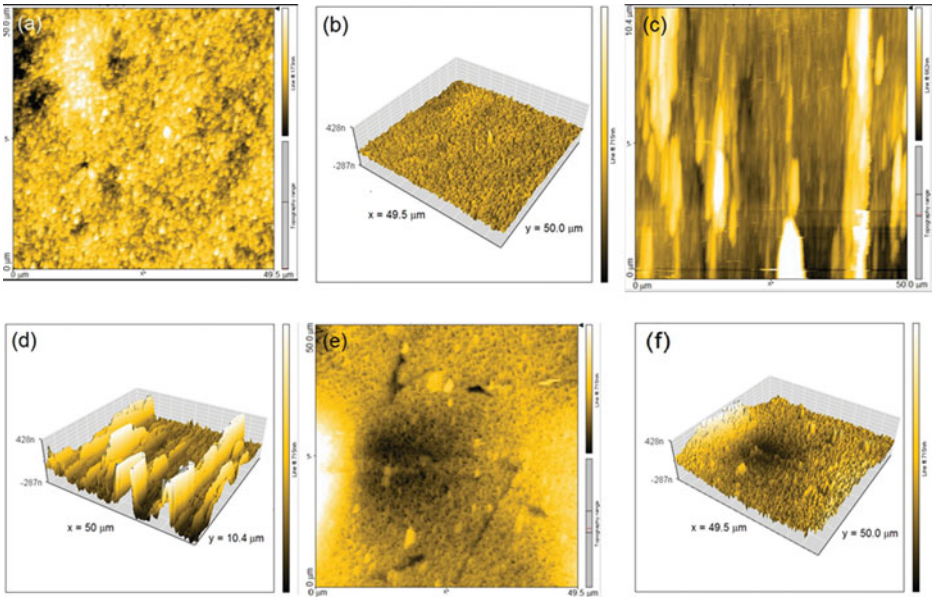


**Figure 5.** AFM surface images of glass/FTO//$TiO_2$ (a,b), glass/FTO/$TiO_2$/$DNA_A$ (c,d) and glass/FTO/$TiO_2$/$DNA_O$ (e,f).

increased reflectance and/or a decreased absorbance influences negatively the DSSC conversion efficiency [44].

Figure 5 shows the AFM images of FTO/$TiO_2$, FTO/$TiO_2$/$DNA_A$, and FTO/$TiO_2$/$DNA_O$ surfaces. Analyzing the images one can see that the smooth surface of ITO (not shown here) becomes regularly rough after deposition of $TiO_2$ with roughness of 28.5 nm (Figure 5a). The addition of DNA results in a formation of plates and some hills [45, 46] evidenced in Figure 5b and c. The FTO/$TiO_2$/$DNA_A$ and FTO/$TiO_2$/$DNA_O$ samples show roughness of 119.7 and 164.5 nm, respectively. As observed in the AFM images addition of DNA results in an increase by 44.8 nm of the sample's roughness and loss of the uniformity. Even though the roughness of the samples increased, the total active area of covered microporous $TiO_2$ decreased due to the formation of continues membrane by DNA samples. This probably negatively influenced the charge transfer in the DSSC.

As mentioned above the series and shunt resistances, non-ideal diode parameters, $TiO_2$-DNA effective area lower when compared with only $TiO_2$ area, DNA-based coating thickness, and porosity can negatively influence the fill factor and consequently device performance. It was shown that the roughness of the $TiO_2$-DNA was higher when compared with only $TiO_2$ coating, which probably influenced a decrease of DSSC solar efficiency. On the another hand, the thickness and porosity of the $TiO_2$-DNA samples is difficult to measure; however, series and shunt resistances are higher for $DNA_O$ than for $DNA_A$. Moreover, the addition of PEDOT:PSS to the $DNA_O$ and $DNA_A$ promoted a decrease and an increase of $R_s$ and $R_{sh}$, respectively.

## Conclusions

The present work describes the results of preparation, characterization and application of DNA and DNA-PEDOT:PSS coatings as HTM in small dye sensitized solar cells. The samples were analyzed throughout impedance, UV-Vis and microscopic measurements. The ionic

conductivities values of the $DNA_O$ samples were of $2.5\times10^{-5}$ and $1.6\times10^{-3}$ S/cm at 25 and 75°C, respectively. The addition of PEDOT:PSS complex to the samples compositions resulted in lower ionic conductivities in the temperature above 45°C. Moreover, it was observed that the ionic conductivity of the DNA and DNA with 2% of PEDOT:PSS increased about two orders of magnitude from *ca* $10^{-5}$ to $10^{-3}$ S/cm when heated from room temperature to 75°C. For the other samples, only one order of magnitude increase was observed. A decrease of the ionic conductivities of the samples of DNA-PEDOT:PSS, when compared with pure DNA membrane was explained in terms of an increase of the samples crystallinity. The transmittance analysis revealed that the samples of DNA are transparent and an addition of PEDOT:PSS promoted a decrease of the transmittance. The DNA-2%PEDOT:PSS displayed transmittance of 62% at 550 nm. This low value is due to the presence PEDOT:PSS that provided a blue coloration to the membranes. The samples were used as HTM in a small DSSC. A decrease of conversion efficiency of these devices was observed when compared with those without DNA. Among the studied DSSCs with DNA coatings, the best conversion efficiency of 0.56% was obtained for those with $DNA_A$. This phenomenon was analyzed by series and shunt resistances values and reflectance analysis. It was observed an increase of reflectance of the samples, which promoted a decrease of absorbance and consequently a decrease of conversion efficiency. Additionally, the samples were studied by the AFM that revealed a change in the topography and roughness of the samples. This probably influenced negatively the charge transfer and redox pair recombination in the studied DSSCs. In summary, the addition of DNA and DNA-PEDOT:PSS as HTM in DSSC promoted a decrease of the conversion efficiency of the device. It was proved that this is due to the change of $TiO_2$-DNA morphology and increase of the device reflectance.

## Acknowledgments

The authors are indebted to FAPESP, CNPq (grant 201820/2014-5), CAPES, European Community for FP7-PEOPLE-2009-IRSES Biomolec – 247544, and STATOIL for the financial support given to this research.

## References

[1] Oregan, B., & Gratzel, M. (1991). *Nature*, *353*, 737.
[2] de Freitas, J. N., Longo, C., Nogueira, A. F., & De Paoli, M. A. (2008). *Sol. Energ. Mat. Sol. Cells*, *92*, 1110.
[3] Kang, M. G., Park, N.-G., Park, Y. J., Ryu, K. S., & Chang, S. H. (2003). *Sol. Energ. Mat. Sol. Cells*, *75*, 475.
[4] Flores, I. C., de Freitas, J. N., Longo, C., De Paoli, M. A., Winnischofer, H., & Nogueira, A. F. (2007). *Journal of Photochemistry and Photobiology a-Chemistry*, *189*, 153.
[5] Kroon, J. M., Grätzel, N. J. B. M.. (2007). *Research and Applications*, *15*, 1.
[6] Lagref, J.-J., Nazeeruddin, M. K., & Grätzel, M. (2008). *Inorganica Chimica Acta*, *361*, 735.
[7] Peter, K., Wietasch, H., Peng, B., & Thelakkat, M. (2004). *Applied Physics A*, *79*, 65.
[8] Tengstedt, C., Crispin, A., Hsu, C.-H., Zhang, C., Parker, I., Salaneck, W. R., & Fahlman, M. (2005). *Organic Electronics*, *6*, 21.
[9] Lorcks, J. (1998). *Polym. Degrad. Stab.*, *59*, 245.
[10] Fink, H. W., & Schonenberger, C. (1999). *Nature*, *398*, 407.
[11] Gullu, O., Cankaya, M., Baris, O., & Turut, A. (2008). *Appl. Phys. Lett.*, *92*.
[12] Kawabe, Y., Koyama, T., & Ogata, N. (2002). *Proc. Soc. Photo-Opt. Inst.*, *4464*, 248.
[13] Andrade, J. R., Raphael, E., & Pawlicka, A. (2009). *Electrochim. Acta*, *54*, 6479.
[14] Mîndroiu, M., Zgârian, R. G., Kajzar, F., Rău, I., De Oliveira, H. C. L., Pawlicka, A., & Tihan, G. T. (2014). *Ionics*, *21*, 1381.

[15] Leones, R., Rodrigues, L. C., Pawlicka, A., Esperanca, J. M. S. S., & Silva, M. M. (2012). *Electrochem. Comm.*, *22*, 189.
[16] Ohno, H., & Takizawa, N. (2000). *Chem. Lett.*, *29*, 642.
[17] Firmino, A., Grote, J. G., Kajzar, F., M'Peko, J.-C., & Pawlicka, A. (2011). *J. Appl. Phys.*, *110*, 033704.
[18] Ohno, H., & Nishimura, N. (2001). *J. Electrochem. Soc.*, *148*, E168.
[19] Leones, R., Esperança, J. M. S. S., Pawlicka, A., de Zea Bermudez, V., & Silva, M. M. (2015). *J. Electroanal. Chem*
[20] Bandyopadhyay, A., Ray, A. K., & Sharma, A. K. (2007). *J. Appl. Phys.*, *102*.
[21] Wang, Y. H., Liu, Y., Yang, H. X., Wang, H., Shen, H., Li, M., & Yan, J. (2010). *Curr. Appl. Phys.*, *10*, 119.
[22] Nithiyanantham, U., Ramadoss, A., Ede, S. R., & Kundu, S. (2014). *Nanoscale*, *6*, 8010.
[23] Zhang, X. L., Liu, J. H., Li, S. M., Tan, X. H., Zhang, J. D., Yu, M., & Zhao, M. G. (2013). *Journal of Materials Chemistry A*, *1*, 11070.
[24] Mindroiu, M., Manea, A.-M., Rau, I., Grote, J. G., Oliveira, H. C. L., Pawlicka, A., & Kajzar, F. (2013). *SPIE*, *8882*, 888202.
[25] Rau, I., Grote, J., Kajzar, F., & Pawlicka, A. (2012). *Comptes Rendus Phys.*, *13*, 853.
[26] Pawlicka, A., Sentanin, F., Firmino, A., Grote, J. G., Kajzar, F., & Rau, I. (2011). *Synth. Met.*, *161*, 2329.
[27] Hagen, J. A., Li, W., Steckl, J., & Grote, J. G. (2006). *Appl. Phys. Lett.*, *88*.
[28] Hirata, K., Oyamada, T., Imai, T., Sasabe, H., Adachi, C., & Koyama, T. (2004). *Appl. Phys. Lett.*, *85*, 1627.
[29] Law, C., Pathirana, S. C., Li, X., Anderson, A. Y., Barnes, P. R., Listorti, A., & Ghaddar, T. H. (2010). *Advanced Materials*, *22*, 4505.
[30] Benedetti, J. E. (2010). Preparação, caracterização e aplicação de eletrólitos polímericos gel em células solares TiO2/corante, in: *Instituto de Quimica Unicamp, Universidade de Campinas- Unicamp*, Campinas, p. 216.
[31] Albinsson, I., Mellander, B.-E., & Stevens, J. (1993). *Solid State Ionics*, *60*, 63.
[32] Firmino, A., Grote, J., Kajzar, F., MPeko, J.-C., & Pawlicka, A. (2011). *Journal of Applied Physics*, *110*, 033704.
[33] Pawlicka, A., Sentanin, F., Firmino, A., Grote, J. G., Kajzar, F., & Rau, I. (2011). *Synthetic Metals*, *161*, 2329.
[34] Zoppi, R. A., & Nunes, S. P. (1997). *Polímeros*, *7*, 27.
[35] Kreuer, K. D. (1996). *Chem. Mater.*, *8*, 610.
[36] Kreuer, K. D. (1997). *Solid State Ionics*, *97*, 1.
[37] Liew, C.-W., & Ramesh, S. (2015). *Carbohydrate Polym.*, *124*, 222.
[38] Mattos, R. I., Pawlicka, A., Lima, J. F., Tambelli, C. E., Magon, C. J., & Donoso, J. P. (2010). *Electrochim. Acta*, *55*, 1396.
[39] Pawlicka, A., Mattos, R. I., Tambelli, C. E., Silva, I. D. A., Magon, C. J., & Donoso, J. P. (2013). *J. Membrane Sci.*, *429*, 190.
[40] Benedetti, J. E., de Paoli, M. A., & Nogueira, A. F. (2008). *Chemical Communications*, 1121.
[41] Bowden, S., & Rohatgi, A. (2001). Proc. 17th European Photovoltaic Solar Energy Conference and Exhibition, Munich, Germany, October 22–26, 2001.
[42] Zhu, K., Kopidakis, N., Neale, N. R., van de Lagemaat, J., & Frank, A. J. (2006). *J. Phys. Chem. B*, *110*, 25174.
[43] Barbe, C. J., Arendse, F., Comte, P., Jirousek, M., Lenzmann, F., Shklover, V., & Gratzel, M. (1997). *Journal of the American Ceramic Society*, *80*, 3157.
[44] Nogueira, A. F. (2001). *Celulas solares de" Gratzel" com eletrolito polimerico, in: Instituto de Qumica de Unicamp*, Universidade de Campinas-UNICAMP, Campinas, p. 171.
[45] Rothemund, P. W. (2006). *Nature*, *440*, 297.
[46] Yengel, E., Wangb, L., Ozkana, M., & Ozkanb, C. S. (2009). *Proc. Proc. of SPIE*.